

Models for Synchrophasor With Step Discontinuities in Magnitude and Phase: Estimation and Performance

Marcelo B. Martins^{ID}, Renata T. de Barros e Vasconcellos^{ID}, and Paulo A. A. Esquef^{ID}, *Member, IEEE*

Abstract—This paper proposes models for the reference phasor in the context of phasor measurement unit calibration, under conditions of step discontinuities in magnitude and phase, along with methods to estimate the model parameters. Two parametric mathematical models, which are proposed to represent these signals, are fitted to signal samples via an iterative numerical method. The proposed approach does not require any time adjustment of the analysis window to skip the discontinuity. The estimated parameters can be used to calculate the frequency, the magnitude, and the phase during magnitude or phase steps. During a window with the step transient, we propose reference phasors with an appropriate definition. Moreover, we quantify the errors of the phasor-related estimates, for both computer-simulated cases and laboratory measurements.

Index Terms—Calibration, dynamic tests, phasor measurement units (PMUs), synchrophasor, uncertainty.

I. INTRODUCTION

THE dynamic behavior of modern electric grid demands testing the performance of phasor measurement units (PMUs) under magnitude and phase steps, as prescribed in the IEEE standard [1], along with its amendment [2]. The accuracy of those measurements depends on the reference values provided by PMU calibration systems. Recent developments in the calibration of PMUs for distribution grids demand lower uncertainty levels than the current systems, designed for the context of transmission grids [3]. The calibration process depends on generating and sampling synchronized waveforms, from which reference phasors are compared to the values provided by the PMU under test. A synchrophasor is the phasor whose phase is the angle relative to an ideal cosine function at the nominal system frequency with a time base synchronous to the Universal Time Coordinated (UTC) [1]. PMUs also provide estimates of the phasor frequency and the rate of change of frequency (ROCOF) at a given reporting rate.

Manuscript received July 9, 2018; revised December 26, 2018; accepted December 29, 2018. Date of publication February 7, 2019; date of current version May 10, 2019. The Associate Editor coordinating the review process was Michael Lombardi. (Corresponding author: Marcelo B. Martins.)

M. B. Martins and R. T. de Barros e Vasconcellos are with the Brazilian National Institute of Metrology, Quality and Technology, Duque de Caxias 25250-020, Brazil (e-mail: mbmartins@inmetro.gov.br; rbvasconcellos@inmetro.gov.br).

P. A. A. Esquef is with the National Laboratory for Scientific Computing, Ministry of Science, Technology, Innovations, and Communications, Petrópolis 25651-075, Brazil (e-mail: pesquef@lncc.br).

Color versions of one or more of the figures in this paper are available online at <http://ieeexplore.ieee.org>.

Digital Object Identifier 10.1109/TIM.2019.2893716

Methods to estimate parameters of signal models with steady-state (SS) or slowly varying frequency, magnitude, or phase, for PMU calibration purposes, are presented in [3] and [4]. Typical variations in parameters or nonlinearities can be modeled by low-order Taylor series expansion. Then, iterative procedures are used to estimate the model parameters.

In previous works [5], [6], the usual approach to deal with transient signals is to ignore the measurements from windows containing disturbances, identified by a transient detector [7]–[9]. This workaround can become inappropriate with the evolution of the electric grid. One example is a recent report of measurement errors during fast transients (a few cycles) that caused the protection system of a solar power plant to cut it off the grid [10]. Such occurrences point out the need for a deeper investigation on measurement errors during fast transients.

In the specific case of an observed phasor disturbed by a step discontinuity in magnitude or phase, the estimation using an underlying SS model does not guarantee convergence nor accuracy [11], [12]. To overcome this difficulty, the method used in [4] adjusts the timestamp and position of the analysis window to skip the discontinuity and sets the phasor estimates where the discontinuity occurs as those obtained from the previous or following window. That way, it avoids the mathematical modeling of a step discontinuity and considers the reference value coming from the SS estimate.

The mentioned procedures are designed to calibrate PMUs and possibly not accurate enough to evaluate the performance of calibration systems. Methods for a more detailed analysis of calibration systems under step conditions are proposed by Frigo *et al.* [13], where the authors used an underlying mathematical model for the transient and a nonlinear (NL) least-squares (LS) method estimator, which showed to outperform state-of-the-art methods, such as the enhanced interpolated discrete Fourier transform (DFT) [14] and the compressive sensing-based Taylor Fourier model [15], when submitted to the IEEE standard tests [1].

This paper extends the preliminary investigation reported in [16] and aims at having accurate phasor estimates under transient conditions. In this context, the following contributions are offered.

- 1) Models that extend those used in Frigo *et al.* [13] in order to account for the time location and the height of the step discontinuity in magnitude or phase,

incorporating representations of both types of transients and the underlying stationary phasor.

- 2) Ways to estimate the model parameters, by:
 - a) using the instantaneous frequency (IF) of Hilbert's analytic signal representation of the phasor, to estimate the location of the step in time;
 - b) using an NL-LS method to estimate the other model parameters (see Section II).
- 3) Proposition of model-based intermediate phasor estimates for step discontinuity situations, which can be used as reference values for PMU calibrations and easily implemented in the existing systems, in place of traditional estimation schemes.
- 4) Monte Carlo quantitative assessment of the errors in the model parameter estimates in function of a range of different:
 - a) signal-to-noise ratio (SNR) levels of the test signals;
 - b) time locations of the step.
- 5) Evaluation of the total vector error (TVE) performance of a simulated DFT-based PMU considering two distinct phasor references.
- 6) Evaluation of a laboratory system intended to be a PMU calibrator based on the aforementioned methods.

As regards item 1, we will show in Section III-B that our proposed models offer phasor-related estimates with lower errors than those reported in [13]. Moreover, concerning item 3, we shown in Section III-D that a simulated DFT-based PMU yields way lower TVEs with respect to our proposed intermediate reference phasors than with respect to usual phasor references based on relocated analysis windows.

In addition to this introduction, this paper is organized as follows. In Sections II-A and II-B, we present the proposed models for dynamic signals with magnitude or phase steps; and the related intermediate phasor definitions. In Sections II-C and II-D, respectively, we describe the proposed detector for the time location of the step and the formulation of the NL-LS estimator for the remaining model parameters. In Section III, we describe the Monte Carlo simulations we run to analyze the numerical errors of each model estimation method. In Section IV, we detail the laboratory measurements devised to evaluate the use of the proposed system for PMU calibration. Finally, in Section V, we discuss the attained results and draw conclusions on the reported investigation.

II. MATHEMATICAL BACKGROUND

A. Mathematical Models for Dynamic Signals

A pure sinusoidal waveform with one magnitude step, located at $t = \tau$, can be modeled in continuous time by

$$y_m(t) = x_1[1 + x_2u(t - \tau)] \cos(\omega t + \phi) + \eta(t) \quad (1)$$

where $u(t)$ is the step function. A similar model for the phasor waveform with one phase step located at $t = \tau$ is

$$y_p(t) = x_1 \cos(\omega t + \phi + x_3u(t - \tau)) + \eta(t) \quad (2)$$

where x_1 is the signal nominal magnitude, x_2 is a decimal value representing the magnitude change, x_3 is the amplitude

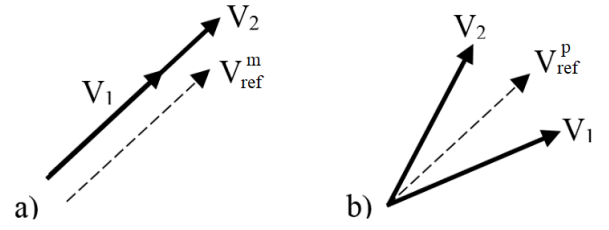


Fig. 1. Intermediate phasors for (a) magnitude step and (b) phase step.

of the phase step, ω is the angular frequency, ϕ is the initial phase, and $\eta(t)$ represents interfering noise. Provided a sufficiently accurate estimate of τ , the set of parameters $\mathcal{P} = \{x_1, x_2, x_3, \omega, \phi\}$ can then be adjusted to obtain a waveform that best fits the data received by the calibration system sampler.

Given a prescribed SNR in decibels, for a zero-mean Gaussian white noise, the noise variance is

$$\eta_0 = \left(\frac{\sigma_y}{10^{\frac{\text{SNR}}{20}}} \right)^2 \quad (3)$$

where σ_y is the standard deviation of the signal $y(t)$.

B. Reference Phasor Values

The IEEE standard [1] prescribes the TVE as the metric to quantify the accuracy of a phasor estimate over a finite analysis window. For that, one compares the estimated phasor with a reference phasor value. In the specific case of signals containing steps at known locations, the reference values are considered undefined, but previous works [4], [13] usually take them from adjacent windows.

In a signal window featuring a step, we propose defining the reference phasors by (4) and (5), which can be evaluated either for *a priori* knowledge of the model parameters of (1) and (2) or estimates of their values by a number of available methods. Following the footsteps of Frigo *et al.* [13], we are going to use the Levenberg–Marquardt (LM) estimator (described in Section III-B), since it does not require analysis from adjacent windows.

The concept of the intermediate reference phasors is illustrated in Fig. 1, where V_1 and V_2 represent, respectively, the SS phasors before and after the step, \hat{V}_{ref}^m and \hat{V}_{ref}^p are, respectively, intermediate phasors that represent the intermediate states during the window with a magnitude or phase step (in Fig. 1(a), \hat{V}_{ref}^m is depicted off-axis only for visualization purposes).

In an observation window with duration T , denoting \hat{x} as an estimate of x , for the magnitude step case with parameters of (1), the estimated intermediate phasor we propose is

$$\hat{V}_{ref}^m = \frac{1}{\sqrt{2}} \frac{\hat{x}_1 \hat{\tau} + \hat{x}_1(1 + \hat{x}_2)(T - \hat{\tau})}{T} \angle \hat{\phi} \quad (4)$$

and the phase step case with parameters of (2), the intermediate phasor we propose is

$$\hat{V}_{ref}^p = \frac{\hat{x}_1}{\sqrt{2}} \angle \frac{\hat{\phi} \hat{\tau} + (\hat{\phi} + \hat{x}_3)(T - \hat{\tau})}{T}. \quad (5)$$

C. Estimation of τ via the Instantaneous Frequency

Hilbert transform has been used to estimate IF of narrowband monocomponent signals, which is the case of ideal electric network phasor components. There are various applications of IF estimation reported in the literature, e.g., characterization of electric disturbances [17] and detection of edits in audio signals that bear the electric network frequency [18]. Anomalous perturbations on the IF can flag the occurrence of discontinuities in the signal.

Given a narrowband monocomponent signal $x(t)$, $t, x \in \mathbb{R}$, let $z(t)$ be the analytic signal associated with $x(t)$, defined as

$$z(t) = x(t) + j\tilde{x}(t) \quad (6)$$

where

$$\tilde{x}(t) = H\{x(t)\} = \int_{-\infty}^{+\infty} \frac{x(u)}{\pi(t-u)} du \quad (7)$$

is the Hilbert transform of $x(t)$. If $z(t)$ is expressed in the polar form

$$z(t) = A(t)e^{j\theta(t)} \quad (8)$$

with $A(t)$ and $\theta(t)$ being, respectively, the instantaneous magnitude and frequency, the IF can be defined as

$$f_i(t) = \frac{1}{2\pi} \frac{d\theta(t)}{dt}. \quad (9)$$

The time discretization of $x(t)$, represented by $x[n]$, gives the discrete version of the analytic signal

$$z[n] = x[n] + jH\{x[n]\}. \quad (10)$$

With discrete version of $H\{x[n]\}$ obtained via fast Fourier transform [19], the discrete IF can be estimated by the numerical derivation with respect to time of the discrete instantaneous phase angle $\theta[n]$. Let $d[n]$ be a detection signal, given by

$$d[n] = |f_i[n]| - m(f_i[n]) \quad (11)$$

where $m(f_i[n])$ is the median value of the sequence $f_i[n]$. As demonstrated in [18], a waveform discontinuity in $x[n]$ manifests as anomalous variations in $d[n]$. Its time location can be detected via appropriate threshold schemes applied to $d[n]$. Here, a similar detection scheme will be used to estimate the parameter τ for the models (1) and (2). Two examples of the detection signal time aligned with the real signal are shown in Figs. 2 and 3, respectively, for magnitude and phase steps, where the circle highlights the step location.

For the sake of simplicity, in the simulations and experiments, we will consider that a discontinuity step is always present. Therefore, τ will be estimated simply as the instant at which the global maximum of $d[n]$ occurs, after discarding the transients at the beginning and end of $d[n]$. Detecting whether there is or not a discontinuity in the input signal is not the purpose here. Nevertheless, it could be accomplished by using appropriate thresholding schemes [18].

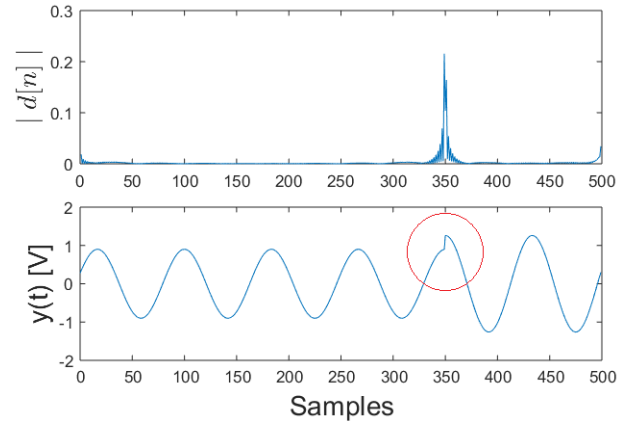


Fig. 2. Detection signal $d[n]$ (top plot) associated with a phasor waveform with magnitude step (bottom plot) ($\tau = 70\%$ of window duration).

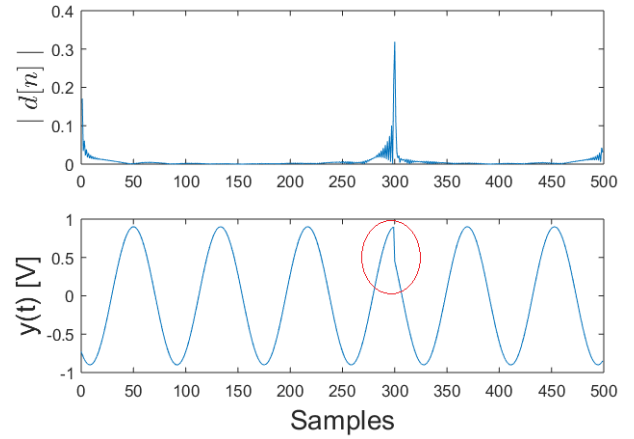


Fig. 3. Detection signal $d[n]$ (top plot) associated with a phasor waveform with phase step (bottom plot) ($\tau = 60\%$ of window duration).

D. Model Parameters Estimation via Levenberg–Marquardt

Let $\hat{y}(k\Delta t)$ be a sequence obtained by evaluating the continuous models (1) or (2) at time instants $t = k\Delta t$, with $k \in \mathbb{Z}$; and $y(k)$ a digital signal which can be either generated via computational simulation or sampled from measured real phenomenon, with uniform sampling period Δt . One wishes to fit N samples of $\hat{y}(k\Delta t)$ with parameters \mathcal{P} to $y(k)$. For that, one can define the error cost function as

$$\epsilon(\mathcal{P}) = \frac{1}{2} \sum_{k=1}^N (y(k) - \hat{y}(k\Delta t))^2 \quad (12)$$

and try to solve the minimization problem $\min_{\mathcal{P}} \epsilon(\mathcal{P})$.

For phasors with slowly varying frequency, low-order Taylor linearization techniques can be used to solve the LS problem [12]. For steplike transient variations, more powerful and costly NL minimization tools, e.g., the LM method [20], [21], are more appropriate [13], [22].

The LM algorithm [20], [21] is an iterative technique for NL minimization problems. It combines the Gauss–Newton method and the steepest descent, being very useful when the size of the descendant step cannot be obtained in a closed form. Instead, numerical approximations of the Jacobian

TABLE I

NOMINAL VALUES AND UNCERTAINTIES USED IN THE SIMULATIONS

Parameter	x_1	x_2	x_3	$\omega/2\pi$	$\phi/2\pi$
Nominal	1 V _p	$\pm 0, 1$	$\pm 10^\circ$	60 Hz	$360^\circ, \pm 120^\circ$
U[%]	1	1	1	0.05	1

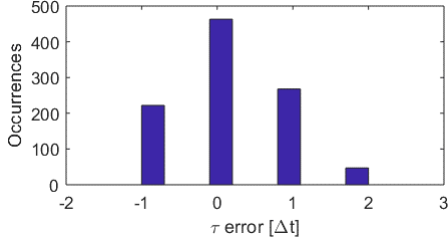


Fig. 4. Histogram of errors in step instant estimation.

matrix are used to estimate the gradient of the cost function and establish an optimal direction. Such NL-LS methods can reach local minima and need a convex cost function, provided by (12).

III. NUMERICAL SIMULATIONS

We performed Monte Carlo simulations with 1000 runs for each setup, to measure the errors between the reference values (of the signal generating model) and those obtained by the computer-based estimators.

For each run, the input signals were digitally generated by evaluating (1) and (2) at $t = k\Delta t$ over a duration of 0.1 s, with $\Delta t = 1/5000$ s, i.e., 5-kHz sampling frequency. The model parameters were set as prescribed in the standard [1], with nominal values and associated uncertainties $U[\%]$ as summarized in Table I.

A. Estimation of τ via Hilbert Analytic Signal

In a simulation, designed to represent a realistic situation, for a window of duration T , we set $\tau \in [0.05T, 0.95T]$ and we allowed 500- $\mu\text{Hz}/\text{Hz}$ variation in frequency and 1% variation in the other parameters, all under a uniform distribution. The maximum errors obtained are not greater than $2\Delta t$ for a SNR > 75 dB, with $\eta(\cdot)$ drawn from zero-mean white Gaussian noise. The histogram of τ errors (in Δt units) for positive magnitude steps of 10% is shown in Fig. 4. Similar histograms were obtained for negative magnitude steps and phase steps of $\pm 10^\circ$.

B. Parameter Estimation With Nonlinear Least Squares

For the uncertainty analysis reported in this section, at each Monte Carlo run, 500 samples of the signal $y(k)$ are generated with uncertainties added to the parameters, drawn from a uniform distribution centered in the nominal values, as shown in Table I, along with additive white Gaussian noise at different SNR levels. Maximum errors of $\pm 2\Delta t$ in the estimation of τ are also simulated. The intermediate phasor magnitude and

TABLE II

STANDARD DEVIATION OF NUMERICAL ERRORS FOR MAGNITUDE STEPS

SNR [dB]	60	93
Frequency [$\mu\text{Hz}/\text{Hz}$]	4.5	0.1
Intermediate Magnitude [$\mu\text{V}/\text{V}$]	47.8	1.0
Phase [m°]	4.6	0.1

TABLE III

STANDARD DEVIATION OF NUMERICAL ERRORS FOR PHASE STEPS

SNR [dB]	60	93
Frequency [$\mu\text{Hz}/\text{Hz}$]	8.4	0.19
Magnitude [$\mu\text{V}/\text{V}$]	46.4	1.0
Intermediate Phase [m°]	5.5	0.11

TABLE IV

PERFORMANCE COMPARISON BETWEEN HLM4 AND LM3

Method Test	HLM4 Magnitude Step	HLM4 Phase Step	LM3 (from [13])
FE [Hz]	$1.6 \cdot 10^{-5}$	$3.2 \cdot 10^{-5}$	$3.5 \cdot 10^{-5}$
TVE [%]	$1.5 \cdot 10^{-3}$	$1.1 \cdot 10^{-3}$	$2.0 \cdot 10^{-3}$

phase are calculated by (4) and (5), respectively. Each estimated quantity is compared to a reference value (perturbed nominal) to obtain the magnitude and phase numerical errors.

In the iterative LM algorithm, the model parameters are initiated at the nominal values, and the optimization procedure seeks for the minimum point of $\epsilon(P)$. In our implementation, iterations are stopped when the convergence criterion $\|\epsilon(P)\| \leq 10^{-10}$ is reached.

The SNR level of about 93 dB used by Frigo *et al.* [13] is desirable for calibration systems. In addition, we performed simulations for 60 dB, to be more realistic with respect to the setup described in Section IV, based on previous work with the same particular equipment [23], [24].

The estimates of the intermediate phasors have substantial lower errors than the initial values, despite having some sensitivity to noise. We report in Tables II and III the standard deviations of the numerical errors of the parameters of interest as well as those of \hat{V}_{ref}^m and \hat{V}_{ref}^p estimates, for SNRs of 60 and 93 dB. As can be seen, with low SNR, the standard deviations of the errors increase, as expected. For both magnitude and phase step tests, the magnitude-related estimates have larger deviations by about one order of magnitude.

C. Comparison With an Alternative Estimator

Hereafter, let HLM4 be the hybrid estimator (see Sections II-C and II-D), we used to obtain the performance figures shown in Tables II and III. Frigo *et al.* [13] report results of an LM estimation scheme (hereafter called LM3) with three parameters $\mathcal{P} = \{x_1, \omega, \phi\}$, being the others assumed to be known *a priori*. They reported performance for step tests in terms of three times the variance of the frequency error (FE) and the highest TVE.

Table IV shows a performance comparison with simulations for SNR = 93.5 dB, under the same basis used by [13], (the reference for TVE is the phasor $x_1 \angle \phi$). One can see that

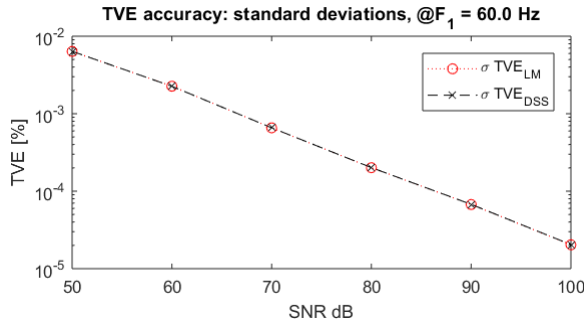


Fig. 5. TVE standard deviations of intermediate phasors: LM versus DSS.

adding the uncertainty in the estimation of τ and one more parameter in the LM estimator related to the depth of the step has little effect on the FE for the phase step case. However, for the magnitude step case, using the HLM4 reduces by half the FE measures. As for the TVE, using the HLM4 yields reductions of about 25% and 45%, respectively, for the magnitude step and phase step cases.

The parameter estimates to calculate intermediate phasors from (4) and (5) can be obtained via standard LS estimators [4, p.1419], from two SS adjacent windows around the step occurrence, as carried out by the National Institute of Standards and Technology (NIST) system [4, p.1419]. We implemented this double steady state (DSS) estimator. One example of magnitude test was simulated, with τ known *a priori*, for different SNR levels. The LM estimator is fed with 1000 samples of the phasor signal containing a step, whereas the DSS estimator takes 500 samples before the step and 500 samples after it. The reference phasor for TVE is calculated from the known parameters used to generate the signals. Fig. 5 shows the standard deviation of TVE versus the SNR level. As can be seen, the LM and DSS estimators yield practically identical TVEs.

D. Influence of Different Reference Phasor Definitions

We performed a computational simulation to show how the definition of reference phasors affects the TVE estimates of a DFT-based PMU. For that, we calculated TVE estimates with two different methods.

- 1) The reference phasors are obtained from a single (the nearest to the step location, known *a priori*) adjacent window of 500 samples, as related in [4], with an SS estimator.
- 2) The reference phasors are estimated from the LM estimator described in Section III-C, with τ known *a priori*.

The simulated PMU receives a signal containing a positive 10% magnitude step, at SNR = 50 dB. The PMU window takes 1000 samples, with a reporting rate of 20 frames/s.

The upper graph of Fig. 6 shows the TVE of the DFT-PMU calculated with method 1 (black line) and method 2 (red line). The lower plot shows the TVE calculated with method 2 alone. As can be seen, phasor references from the LM method produce TVEs under 0.03% against a way higher 5% when the phasor references are from the SS estimator.

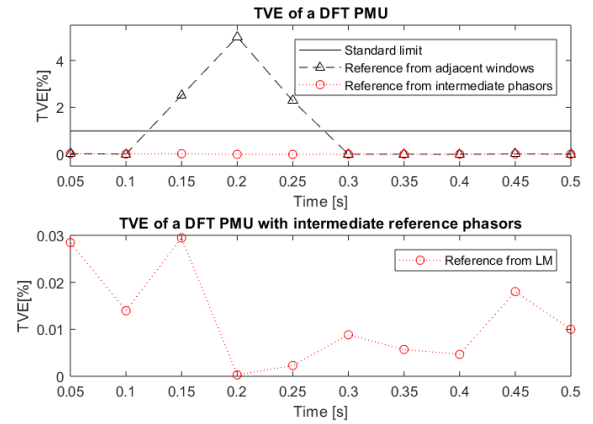


Fig. 6. TVE as calculated with reference phasors estimated from the proposed estimator versus SS method.

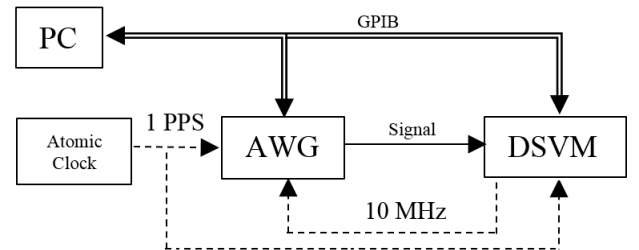


Fig. 7. Diagram of the prototype system.

With the SS method, the time response (TR) from the TVE lasts about 250 ms, and the PMU would be rejected as a P-class. On the other side, with our LM-based phasor reference, the TVE of the DFT-PMU never passes the standard limit.

The large differences in TVE and TR are mainly due to the time displacement of the window used by method 1 to obtain the reference phasors. Our intermediate reference phasors are more stable and smooth along time, despite the step transient, as it takes into account (in a weighted manner) the phasor states before and after the step. This may be potentially useful for the already standardized P-class PMU tests, for possibly more stringent TR tests for distribution PMUs in the future, and for the development of more robust applications for protection systems.

IV. LABORATORY MEASUREMENTS

Aiming at validating the proposed method with real-world signals, we made several measurements using one digital sampling voltmeter (DSVM) and one arbitrary waveform generator (AWG), controlled by a personal computer via general purpose interface bus (GPIB). The connections among the system components can be seen in the block diagram of Fig. 7 and follow the setup used in [25]. In this analysis, we assumed that the uncertainties inserted by the DSVM are negligible in relation to those due to the AWG [23], [24]. The DSVM trigger time delay is one component of the overall phase error (indeed, part of the absolute phase uncertainty, the estimation of which is beyond the scope of this paper), and its influence is part of the variations observed in the results. However, previous work [26] indicates time delays less than 50 ns and jitter less than 100 ps.

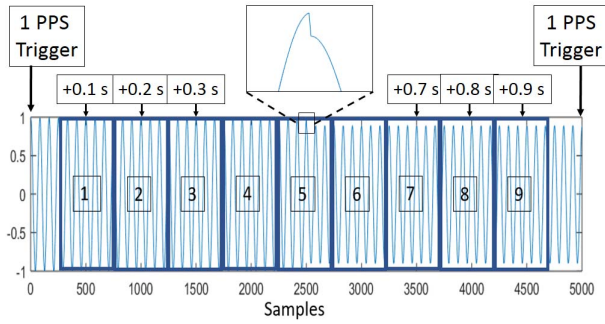


Fig. 8. Magnitude step occurrence in the fifth window.

The same waveforms used in the simulations are set to be reproduced by the AWG, with a nominal output of $1 V_p$, and synchronously sampled by the DSVM. Both are triggered with a 1 PPS signal, coming from an atomic clock, so we can control the initial phase. The internal clock from the DSVM is used as an external 10-MHz reference signal for the generator. 5000 samples are taken during 1 s and stored in the DSVMs internal memory.

For convenience, we set the UTC second at the center of the analysis window, coherent with the UTC second and its decimal fractions. If we set 500 samples/window, we have 10 windows per second. The first window lacks 250 samples before the UTC second. Therefore, it is discarded and the analysis starts at the next window. The center of the first complete window will be coherent with the first 0.1 s after the UTC second, as shown in Fig. 8. Then, we have nine complete windows containing six cycles of 60 Hz each. The steps of magnitude or phase occur in the fifth window. According to the procedure for equivalent sampling prescribed in the standard [1], the steps occur at $\tau_l = 0.1Tl$, $l = 1, 2, \dots, 8, 9$, where T is the duration of a single analysis window, in seconds. In other words, in the fifth window, the steps occur at sample indices $k = 50, 100, 150, \dots, 450$.

For the windows with SS waveforms, the same fitting algorithm reported in [4] is used to obtain the synchrophasors and frequency estimates. For the fifth window, the intermediate phasors were calculated using (4) or (5), from the estimated model parameters of (1) or (2), respectively (see Sections II-C and II-D). The estimates of the step instant were not greater than $2\Delta t$, inside the expected uncertainty. The estimation errors of the other parameters are analyzed in Sections IV-A–IV-C.

A. Intermediate Reference Phasors

The system is capable of providing reference phasors for the fifth window, despite the occurrences of steps in magnitude and phase, as shown in Figs. 9 and 10, respectively. Each series of data shows different step instant occurrences in the fifth timestamp, in percentage of the window period T . As can be seen, the attained results indeed are intermediate phasors and reflect well the weighted models (4) and (5), as functions of τ : the closer τ is to the fourth window, the farther the intermediate phasor resembles that of the fourth window and the closer it gets to the sixth window.

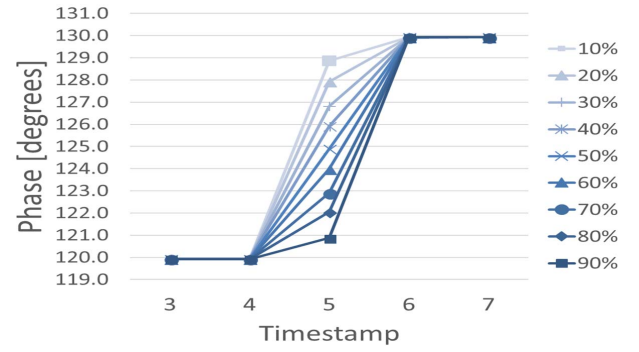


Fig. 9. Phase of the reference phasor (5) for $+10^\circ$ step, with $\phi = 120^\circ$.

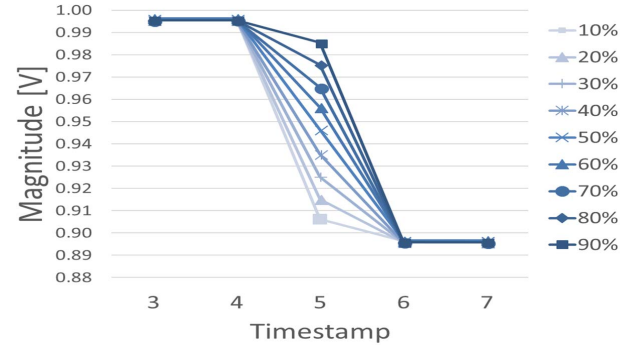


Fig. 10. Magnitude of the intermediate phasor (4) for $x_2 = -0.1$.

Magnitude Step Test: Frequency difference to nominal values [$\mu\text{Hz}/\text{Hz}$]

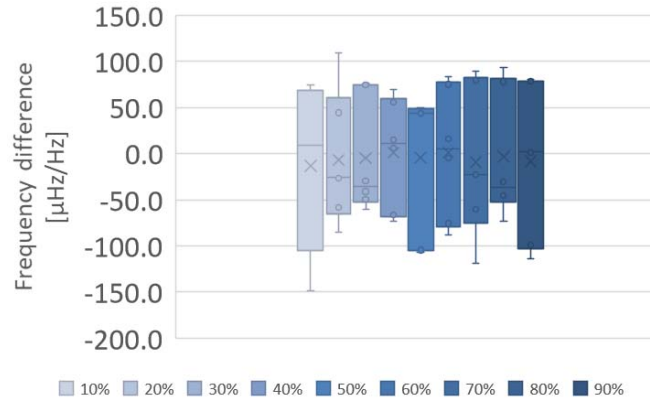


Fig. 11. Frequency difference to nominal value during magnitude tests as function of the step instant, in percentage of T . The bars in the plots represent quartiles.

B. Frequency

Frequency estimates (SS based) for the analysis windows with SS signals have standard deviation no greater than $9 \mu\text{Hz}/\text{Hz}$ (0.5 mHz) from the nominal value. When submitted to magnitude steps, the LM estimates provided by the system have standard deviations from the nominal value of about $70 \mu\text{Hz}/\text{Hz}$ (4 mHz), on average, as shown in Fig. 11, where the values for each plot have been measured for the shown locations of τ in percentage of T .

The largest frequency variations are observed when the system is required to generate and measure phase steps. As shown in Fig. 12, standard deviations of the FEs of about $40 \mu\text{Hz}/\text{Hz}$ (2 mHz) have been measured when the phase

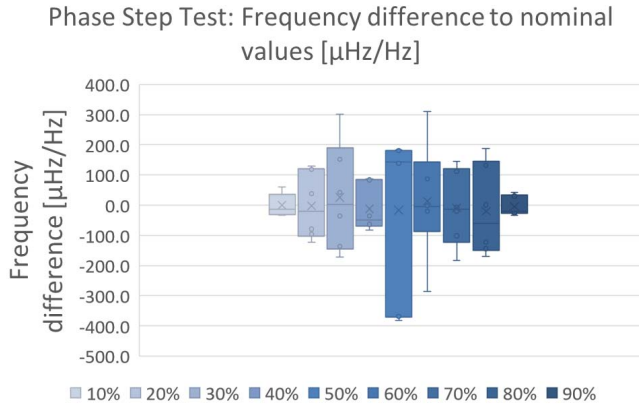


Fig. 12. Frequency difference to nominal value during phase steps as function of the step instant, in percentage of T .

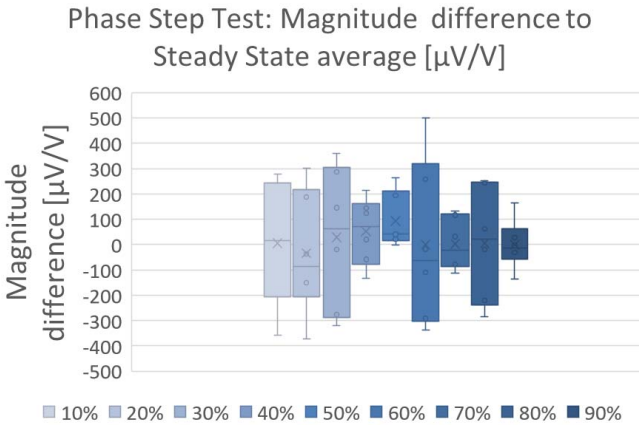


Fig. 13. Magnitude differences to SS average during phase steps as function of the step instant of occurrence.

step occurrence is near the boundaries of the window, and at $\tau = 50\%$, soar to $280 \mu\text{Hz/Hz}$ (17 mHz).

C. Magnitude During Phase Step and Vice Versa

During SS conditions, the magnitude estimates have a standard deviation no greater than $160 \mu\text{V/V}$, whereas the phase estimates have standard deviations of about 1.7 m° .

Ideally, a signal with a magnitude step, see (1), would have unperturbed phase. Similarly, x_1 would be constant for the phase step, see 2. However, in an actual laboratorial experimental setup, perturbations are produced when the AWG is forced to generate a steplike waveform. We quantified the AWG limitations in this challenging scenario.

For example, during a phase step, the magnitude varies as shown in Fig. 13. Similarly, during a magnitude step, the phase varies as shown in Fig. 14. For a phase step test, perturbations in the measured phasor magnitude have a standard deviation of about $200 \mu\text{V/V}$ with respect to the average magnitude value, as measured from the windows with SS phasors.

The estimates of phase during magnitude step tests present higher variations. As shown in Fig. 12, there is a tendency for the standard deviation to increase as the location of the step discontinuity is set near the extremities of the analysis window. The standard deviations have a minimum value of about 10 m° , going up to about 70 m° . Possibly, the higher errors found during transients are due to limitations of the

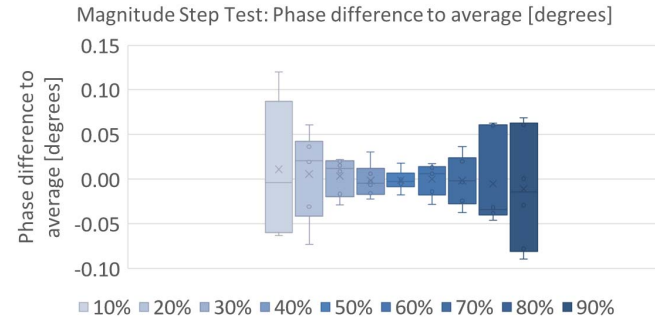


Fig. 14. Phase difference to average during magnitude steps as function of the step instant of occurrence.

AWG in rendering a steplike phase waveform for the phasor, thus degrading the performance of the LM estimator when the step occurs near the extremities of the analysis window.

V. CONCLUSION

Models for phasor signals disturbed by magnitude and phase step discontinuity were proposed, in the context of an assessment of PMU calibration systems in transient conditions, along with related models for intermediate reference phasors for such transient conditions. We present a model-based method to estimate the magnitude and phase of the proposed intermediate phasors, which can be used as references in PMU calibration systems, during magnitude or phase step tests. The method also allows measuring several quantities, such as the phasor frequency; the phasor magnitudes before and after the step; the step depth both in magnitude and phase; and the phasor magnitude during phase step tests (and vice versa).

Estimation of the step location via Hilbert's IF analysis provided accurate results, which aided the estimation of the remaining model parameters via an NL-LS method. The proposed approach tackles the estimation of phasor-related values from an observed perturbed phasor signal, within an analysis window, by ideally modeling the disturbance, instead of discarding it from the analysis. The estimation accuracy of each parameter and intermediate phasor has been measured via computer-simulated setups under different noise conditions and uncertainties forced upon the model parameters used to generate the test signals. Within the the scope of the designed setup of the computer simulation tests, the proposed method can give reliable and accurate results to assess PMU calibration systems.

An analysis of a laboratory system intended to calibrate PMUs has been performed. The experimental results show that, during a steplike transient, parameter errors have higher standard deviations than those observed during an SS. Substantial deviations of frequency, magnitude, and phase during magnitude or phase step tests were detected. We shall note that the AWG we employed generates signals with an estimated SNR of about 60 dB . At this SNR, the standard deviations of the parameter estimation errors, for the computer-generated phasor signals, are about one order of magnitude lower than those measured for the laboratory prototype (compare the results shown in Tables II and III with those of Figs. 12–14). These discrepancies suggest that the AWG SNR alone is insufficient to explain the poorer performance and there are

other factors at play that deserve to be further investigated. Using a less noisy and more stable signal source would help to sort out the question.

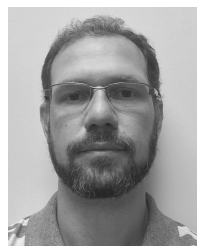
In special situations, the sensitivity of τ estimation can be high with SNR as low as 50 dB. Moreover, it may vary depending on the initial phase, and on the location of τ inside the window. For example, steps occurring very near a zero crossing, as well as local maxima and minima of the phasor waveform are particularly challenging cases. However, a more elaborated detector based on both the IF and magnitude of Hilbert's analytic signal can be implemented to deal with these cases. We leave for a future work reporting the investigation of these challenging cases.

ACKNOWLEDGMENT

M. Martins would like to thank A. Goldstein for the valuable comments and guidelines.

REFERENCES

- [1] *IEEE Standard for Synchrophasor Measurements for Power Systems*, IEEE Standard C37.118.1-2011, Dec. 2011.
- [2] *IEEE Standard for Synchrophasor Measurements for Power Systems—Amendment 1: Modification of Selected Performance Requirements*, IEEE Standard C37.118.1a-2014, Apr. 2014.
- [3] D. Colangelo *et al.*, "Architecture and characterization of a calibrator for PMUs operating in power distribution systems," in *Proc. IEEE Eindhoven PowerTech*, Jul. 2015, pp. 1–6.
- [4] Y. H. Tang, G. N. Stenbakken, and A. Goldstein, "Calibration of phasor measurement unit at NIST," *IEEE Trans. Instrum. Meas.*, vol. 62, no. 6, pp. 1417–1422, Jun. 2013.
- [5] M. H. Bollen and M. H. Bollen, *Understanding Power Quality Problems: Voltage Sags and Interruptions*, vol. 445. New York, NY, USA: IEEE press, 2000.
- [6] A. G. Phadke and J. S. Thorp, *Synchronized Phasor Measurements and Their Applications*. New York, NY, USA: Springer, 2008.
- [7] J. Ren and M. Kezunovic, "An adaptive phasor estimator for power system waveforms containing transients," *IEEE Trans. Power Del.*, vol. 27, no. 2, pp. 735–745, Apr. 2012.
- [8] M. de Apraiz, R. I. Diego, and J. Barros, "Transient detection in phasor measurement units with kalman filtering," in *Proc. 18th Int. Conf. Harmon. Qual. Power (ICHQP)*, May 2018, pp. 1–6.
- [9] J. Barros, M. de Apraiz, and R. I. Diego, "A wavelet-based transient detector for P and M class phasor measurement unit integration," in *Proc. IEEE Int. Workshop Appl. Meas. Power Syst. (AMPS)*, Sep. 2017, pp. 1–6.
- [10] A. J. Roscoe, A. Dyško, B. Marshall, M. Lee, H. Kirkham, and G. Rietveld, "The case for redefinition of frequency and ROCOF to account for AC power system phase steps," in *Proc. IEEE Int. Workshop Appl. Meas. Power Syst. (AMPS)*, Sep. 2017, pp. 1–6.
- [11] A. G. Phadke and B. Kasztenny, "Synchronized phasor and frequency measurement under transient conditions," *IEEE Trans. Power Del.*, vol. 24, no. 1, pp. 89–95, Jan. 2009.
- [12] G. Stenbakken, T. Nelson, M. Zhou, and V. Centeno, "Reference values for dynamic calibration of PMUs," in *Proc. 41st Annu. Hawaii Int. Conf. Syst. Sci.*, Jan. 2008, p. 171.
- [13] G. Frigo, D. Colangelo, A. Derviskadić, M. Pignati, C. Narduzzi, and M. Paolone, "Definition of accurate reference synchrophasors for static and dynamic characterization of PMUs," *IEEE Trans. Instrum. Meas.*, vol. 66, no. 9, pp. 2233–2246, Sep. 2017.
- [14] P. Romano and M. Paolone, "Enhanced interpolated-DFT for synchrophasor estimation in FPGAs: Theory, implementation, and validation of a PMU prototype," *IEEE Trans. Instrum. Meas.*, vol. 63, no. 12, pp. 2824–2836, Dec. 2014.
- [15] M. Bertocco, G. Frigo, C. Narduzzi, C. Muscas, and P. A. Pegoraro, "Compressive sensing of a Taylor-Fourier multifrequency model for synchrophasor estimation," *IEEE Trans. Instrum. Meas.*, vol. 64, no. 12, pp. 3274–3283, Dec. 2015.
- [16] M. B. Martins, "Models for synchrophasor with step discontinuities in magnitude and phase, their parameter estimation and performance," in *Proc. Conf. Precis. Electromagn. Meas.*, Paris, France, Jul. 2018, pp. 1–2.
- [17] M. Caciotta, S. Giarnetti, F. Leccese, and Z. Leonowicz, "Detection of short transients and interruptions using the Hilbert transform," in *Proc. World Congr. Fundam. Appl. Metrol.*, Sep. 2009, pp. 913–916.
- [18] P. A. A. Esquef, J. A. Apolinário, and L. W. P. Biscainho, "Edit detection in speech recordings via instantaneous electric network frequency variations," *IEEE Trans. Inf. Forensics Security*, vol. 9, no. 12, pp. 2314–2326, Dec. 2014.
- [19] L. Marple, "Computing the discrete-time 'analytic' signal via FFT," *IEEE Trans. Signal Process.*, vol. 47, no. 9, pp. 2600–2603, Sep. 1999.
- [20] K. Levenberg, "A method for the solution of certain non-linear problems in least squares," *Quart. J. Appl. Math.*, vol. 2, no. 2, pp. 164–168, Jul. 1944.
- [21] D. W. Marquardt, "An algorithm for least-squares estimation of nonlinear parameters," *J. Soc. Ind. Appl. Math.*, vol. 11, no. 2, pp. 431–441, 1963.
- [22] M. B. Martins, R. M. Debatin, and A. M. R. Franco, "System for metrological assessment of PMUs under voltage sags," in *Proc. 17th Int. Conf. Harmon. Qual. Power (ICHQP)*, Oct. 2016, pp. 535–538.
- [23] W. G. K. Ihlenfeld and R. T. B. Vasconcellos, "A digital four terminal-pair impedance bridge," in *Proc. Conf. Precis. Electromagn. Meas.*, Jul. 2016, pp. 1–2.
- [24] "Agilent 33250a users guide," Agilent Technol., Loveland, CO, USA, Tech. Rep. 33220-90002, 2005.
- [25] R. T. de Barros e Vasconcellos, V. R. de Lima, W. G. K. Ihlenfeld, and F. D. Silveira, "Coaxial and digital impedance bridges for capacitance measurements at the nF range," *IEEE Trans. Instrum. Meas.*, vol. 66, no. 6, pp. 1553–1559, Jun. 2017.
- [26] U. Pogliano, "Use of integrative analog-to-digital converters for high-precision measurement of electrical power," *IEEE Trans. Instrum. Meas.*, vol. 50, no. 5, pp. 1315–1318, Oct. 2001.



power, energy, power quality, and synchrophasor measurements.



the Electrical Standardization Metrology Laboratory. Her current research interests include electrical metrology in general, and high-accuracy impedance measurements in particular, and digital sampling techniques applied to electrical metrology.



communications, Petrópolis, Brazil. His current research interests include digital signal processing and related applications to audio and acoustical signal processing, analysis, synthesis, and modeling of electrical signals.

Mr. Esquef is a member of the Audio Engineering Society.

Marcelo B. Martins received the B.E. degree in electrical engineering and the M.Sc. degree in electrical engineering from the Federal University of Minas Gerais, Belo Horizonte, Brazil, in 2007 and 2010, respectively. He is currently pursuing the Ph.D. degree with the National Laboratory of Scientific Computing, Petrópolis, Brazil.

In 2012, he joined the Brazilian National Institute of Metrology, Quality and Technology, Duque de Caxias, Brazil, where he has been involved in digital signal processing and electrical metrology applied to

Renata T. de Barros e Vasconcellos was born in Rio de Janeiro, Brazil, in 1976. She received the B.E. degree in electrical engineering from the Federal University of Rio de Janeiro (UFRJ), Rio de Janeiro, Brazil, in 2000, the M.Sc. and D.Sc. degrees in electrical engineering from Instituto Alberto Luiz Coimbra de Pós-Graduação e Pesquisa em Engenharia (COPPE)/UFRJ, in 2002 and 2012, respectively.

In 2002, she joined the Brazilian National Institute of Metrology, Quality and Technology, Duque de Caxias, Brazil, where she is currently the Head of the Electrical Standardization Metrology Laboratory. Her current research interests include electrical metrology in general, and high-accuracy impedance measurements in particular, and digital sampling techniques applied to electrical metrology.

Paulo A. A. Esquef (M'96) received the B.E. degree from the Federal University of Rio de Janeiro (UFRJ), Rio de Janeiro, Brazil, in 1997, the M.Sc. degree in from Instituto Alberto Luiz Coimbra de Pós-Graduação e Pesquisa em Engenharia (COPPE)/UFRJ, in 1999, and the D.Sc. (tech.) degree from Aalto University, Espoo, Finland, in 2004, all in electrical engineering.

He is currently an Adjoint Researcher at the National Laboratory of Scientific Computing, Ministry of Science, Technology, Innovations, and Communications, Petrópolis, Brazil. His current research interests include digital signal processing and related applications to audio and acoustical signal processing, analysis, synthesis, and modeling of electrical signals.